

Giant piezoresistance in silicon-germanium alloysF. Murphy-Armando¹ and S. Fahy²¹*Tyndall National Institute, University College Cork, Lee Maltings, Dyke Parade, Cork, Ireland*²*Tyndall National Institute and Department of Physics, University College Cork, Ireland*

(Received 26 March 2012; revised manuscript received 18 June 2012; published 9 July 2012)

We use first-principles electronic structure methods to show that the piezoresistive strain gauge factor of single-crystalline bulk *n*-type silicon-germanium alloys at carefully controlled composition can reach values of $G = 500$, three times larger than that of silicon, the most sensitive such material used in industry today. At cryogenic temperatures of 4 K we find gauge factors of $G = 135\,000$, 13 times larger than that observed in Si whiskers. The improved piezoresistance is achieved by tuning the scattering of carriers between different (Δ and L) conduction band valleys by controlling the alloy composition and strain configuration.

DOI: [10.1103/PhysRevB.86.035205](https://doi.org/10.1103/PhysRevB.86.035205)

PACS number(s): 72.20.Fr, 72.15.Eb

I. INTRODUCTION

The piezoresistive effect was first reported in metals by Lord Kelvin in 1856,¹ but did not find an application until 80 years later in strain gauges.² With improvements in the semiconductor electronics manufacturing processes, and the discovery in the 1950s that silicon and germanium have a very large piezoresistive effect,³ the field of piezoresistive sensors started to flourish. Today, these sensors have a considerable market share of all microelectromechanical systems (MEMS)-based sensors, with applications that include strain gauges, accelerometers, pressure, force, and inertial sensors, atomic force microscopy, and even data storage.⁴

Nowadays, as applications require ever more sensitive sensors, research to find materials with larger piezoresistive factors is as active as ever. The sensitivity of a piezoresistive sensor is determined by the strain gauge factor, given by $G = \frac{1}{R} \frac{dR}{d\epsilon}$, where R is the resistance and ϵ the strain. The largest ambient temperature G found for single crystalline bulk silicon is $G = 170$,^{3,5} and for germanium $G = 100$.⁶ The state of the art material in the industry is poly-silicon, with $G < 10$, which can be improved to $G \simeq 20$ by using *p*-type poly-SiGe.⁷ Recently, gauge factors of $G \simeq 1000$ were reported for silicon oxycarbonitride polymer-derived ceramic⁵ and a $G = 843$ for a silicon-metal hybrid.⁸ A lot of excitement was produced by the report of giant piezoresistivity in silicon nanowires,^{9,10} with the latest room temperature value reported being $G = 280$.¹¹

The earliest work hinting at a higher piezoresistive effect in *n*-type SiGe alloys of high Ge compositions was performed by R. W. Keyes in 1957.¹² He found a piezoresistive effect 15% larger than in pure Ge at a Ge composition of $x = 0.96$. Unfortunately, at that time the scattering parameters and band-structure of the alloys were unknown, and the suggested effect for the larger piezoresistance was attributed to a large change in deformation potentials with composition, and the possibilities for SiGe as a piezoresistive element have not been further explored.

In this work we use *ab initio* theoretical methods^{13–16} to explore the parameter space in alloy composition, strain configuration, and current direction to determine the best possible strain gauge factors for single crystalline *n*-type bulk silicon-germanium alloys. We find ambient temperature gauge factors as high as $G = 500$, which are a factor of three larger than the maximum possible for single-crystalline silicon, and

over five times that of germanium. At cryogenic temperatures of 4.2 K we find gauge factors between 12 000 and 130 000, 1.2 to 13 times higher than those reported for Si whiskers.¹⁷

Ab initio methods are powerful predictive tools that can compute the behavior of materials without the need of fitting parameters, allowing us to realize the concept of materials by design.¹⁸ In our previous studies^{13–15} we calculated the mobility of silicon germanium at all compositions and found excellent agreement with experiments. These calculations yielded previously unknown scattering and transport parameters that were used to predict the mobility in strained Ge¹⁹ and strained SiGe alloys.¹⁶ Similar *ab initio* methods have also been used to calculate the electron-phonon scattering parameters in Ge,²⁰ GaAs, and GaP,²¹ with excellent agreement with experiments.

II. CALCULATION AND RESULTS

We calculate all the relevant carrier scattering parameters from first principles. The acoustic electron-phonon scattering is calculated using density functional theory (DFT) and the frozen phonon method¹⁵ accounting for the effects of strain on the matrix elements.¹⁶ The intervalley and optical electron-phonon scattering is calculated with density functional perturbation theory, considering the effects of alloy disorder within the random mass approximation.^{15,16} Alloy disorder scattering is calculated using the supercell approach and DFT as reported in Ref. 13. The band energies as a function of strain are calculated using the GW approximation. The conductivity as a function of composition and strain is calculated with the Boltzmann transport equation under the relaxation time approximation. We concentrate on *n*-type doping regimes at which ionized impurity scattering is negligible, viz., $n < 10^{16} \text{ cm}^{-3}$. We corroborate this assumption by including ionized impurity scattering as in the Brooks-Herring approach^{22–24} in the calculation of the mobility. The effective masses for electrons are taken from the calculated energy distribution of the conduction band valleys. All details of the numerical methods used to find the *n*-type mobility in strained and unstrained alloys are given in detail in Refs. 13, 15, and 16 and the various numerical convergence parameters used in this work are the same as used there.

We consider two types of strain (expressed in Miller index notation): (i) an ideal pure uniaxial strain in the [111] direction,

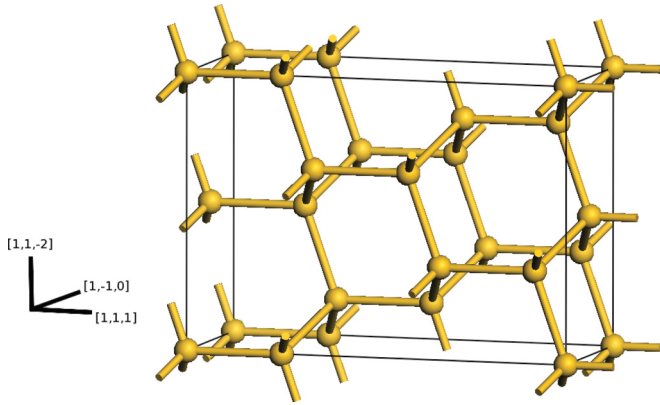


FIG. 1. (Color online) Diamond lattice structure shown along the $[111]$, $[1\bar{1}0]$, and $[1\bar{1}\bar{2}]$ directions.

and (ii) a cantilever-type strain in the $[111]$ direction, relaxing in the $[1\bar{1}\bar{2}]$ direction, with zero strain in the $[1\bar{1}0]$ direction (see Fig. 1). Type (ii) strain is found in cantilevers used in strain gauges and atomic force microscopes. We also consider uniaxial strain in the $[100]$ direction, and find gauge factors similar to those of pure Si and Ge, and are not treated here. We calculate the gauge factor G for varying strain and Ge composition, and for current flowing in the $[111]$ and $[1\bar{1}0]$ directions. Figures 2(a) and 2(b) show the most dramatic results for cases (i) and (ii), namely, with current in the $[111]$ and $[1\bar{1}0]$ directions, respectively. In Fig. 2(a) we observe that the maximum gauge factor is achieved at $x = 0.895$ at zero pre-strain, with $G = 400$. For the more realistic case (ii), shown in Fig. 2(b), the gauge factor at zero pre-strain reaches $G = 150$, increasing to $G = 508$ at $x = 0.88$ with 0.2% compressive pre-strain. The latter type of strain can be achieved by growing the active $\text{Si}_{1-x}\text{Ge}_x$ on a SiGe substrate of lower Ge content. At cryogenic temperatures of 4 K and zero pre-strain and current in the $[111]$ direction, type (ii) strain produces a very narrow peak of $G = -28\,000$ at $x = 0.87$, and drops to $G = -12\,000$ between $0.875 < x < 0.98$. For current along the $[1\bar{1}0]$ direction, the gauge factor reaches $G = 80\,000$ at $x = 0.87$ for a pre-strain of 0.001%, and $G = -135\,000$ at $x = 0.869$ for a pre-strain of 0.014%. The gauge factor for Ge at 4 K for type (ii) strain is $G = 7000$.

III. DISCUSSION

The large piezoresistive effect in this material can be understood by the different conductivity regimes available in a strained SiGe alloy. The conductivity in n -type $\text{Si}_{1-x}\text{Ge}_x$ can be described by an effective mass theory for the movement of the carriers. At Ge compositions $x < 0.87$, conductivity occurs through six degenerate conduction band valleys, located in the Δ crystallographic line along the Cartesian axes in reciprocal space. At compositions $x > 0.87$ there are four conduction band valleys located at the L crystallographic point in the Brillouin zone in reciprocal space, in the $[111]$, and equivalent directions.²⁵ Each of these valleys have anisotropic energy-momentum dispersions: The effective mass along the axis of the valley is larger than perpendicular to it.²⁵ This means that for each valley, the conductivity perpendicular to the direction of the valley will be higher than parallel to it. When all the valleys are degenerate, the total conductivity is an average of that of each valley, and is therefore isotropic. Strain along the axis of one of the valleys breaks this isotropy by lifting the degeneracy of the valleys. The room temperature conductivity of Si is $2\frac{1}{2}$ smaller than that of Ge. In the alloy, as the Ge composition increases, the conductivity is reduced even further by alloy scattering of the carriers, and is lowest at $x = 0.87$, where the 10 conduction valleys are degenerate and intervalley scattering is therefore stronger.¹⁵ Beyond this point the conductivity rapidly increases to reach that of Ge.

The piezoresistive effect is due to a change in conductivity produced by an applied strain. The gauge factor is defined as the fractional change in resistance with strain, and is related to the fractional change in conductivity,²⁶

$$G = \frac{1}{R} \frac{dR}{d\epsilon} \simeq \frac{1}{\rho} \frac{d\rho}{d\epsilon} = -\frac{1}{\sigma} \frac{d\sigma}{d\epsilon}, \quad (1)$$

where ρ and σ are the resistivity and conductivity, respectively. The conductivity is related to the mobility μ as

$$\sigma = en\mu, \quad (2)$$

where n is the total carrier density and e the electron charge. The mobility can be further decomposed into the sum of the

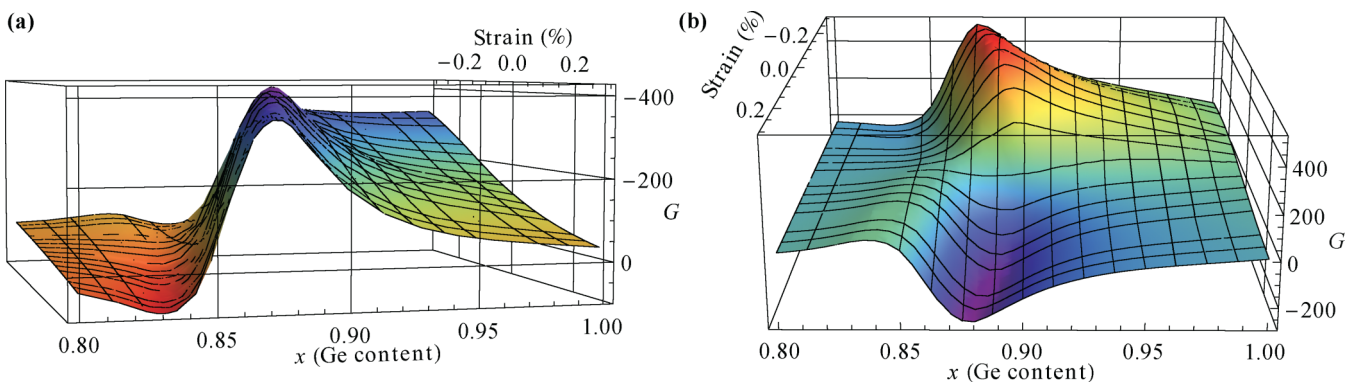


FIG. 2. (Color online) Room temperature piezoresistive strain gauge factor G vs Ge composition x and $[111]$ strain. (a) Strain applied in the $[111]$ direction, with current in the $[111]$ direction. (b) Cantilever-type stress, with strain applied in the $[111]$ direction (clamped in the $[1\bar{1}0]$ direction and relaxed in the $[1\bar{1}\bar{2}]$ direction), with current in the $[1\bar{1}0]$ direction.

contributions by the mobility of each valley,

$$\mu = \sum_i r_i \mu_i, \quad (3)$$

where $r_i = n_i/n$ and μ_i are the relative carrier population and mobility of valley i . Assuming that the total carrier population remains constant under strain, the gauge factor expressed as a function of the mobility of each valley becomes

$$G = -\frac{1}{\mu} \sum_i \left(\mu_i \frac{dr_i}{d\epsilon} + r_i \frac{d\mu_i}{d\epsilon} \right). \quad (4)$$

As the relative energy between valleys changes with strain, so does the relative carrier population of each valley and the intervalley scattering rate, the latter strongly affecting the mobility of each valley. A number of factors may conspire to produce a very high G factor, such as

- (1) at least one valley i with high mobility μ_i (which depends on the current direction),
- (2) a large variation in relative occupation r_i with strain,
- (3) a valley with high relative occupation, and
- (4) a large variation in intervalley scattering (and therefore in mobility) with strain,
- (5) the opposite of all of the above for all other valleys in which the change in mobility and occupation with strain is of opposite sign, and
- (6) a low total mobility.

These factors are present in pure Si and Ge, where the relative occupation and intervalley scattering of the Δ valleys in Si, and the L valleys in Ge can be changed.³ The lower total mobility of Si is one of the reasons the gauge factor is larger than in Ge. In SiGe alloys there are two additional advantages: (a) the total mobility is much lower due to the presence of alloy scattering, and (b) there are 10 valleys to play with, which means that there is an extra variation in intervalley scattering and in relative carrier occupation. We will now illustrate how these factors produce the large gauge factor in type (i) strained SiGe.

The lowest total mobility in SiGe occurs at compositions around $x = 0.87$, when all 10 conduction band valleys are nearly degenerate. However, all the other factors in Eq. (4) are not as favorable as at other compositions. The best combination for this type of strain occurs at $x = 0.895$. At this composition at zero strain, the four L valleys are degenerate, 32 meV below the six Δ valleys. Type (i) strain removes the degeneracy of the L valley into triply ($L3$) and singly ($L1$) degenerate valleys, and leaves the six Δ valleys degenerate. At room temperature, the relative occupation of the $L3$, $L1$, and Δ valleys is 0.44, 0.15, and 0.41, respectively. Tensile (compressive) strain

lowers the $L3$ ($L1$) valleys relative to both the $L1$ ($L3$) and Δ valleys. For a current flowing in the direction of the strain, which coincides with the low conductivity direction of valley $L1$, the relative mobility μ_i/μ of each valley is the following: 1.9, 0.1, and 0.33 for the $L3$, $L1$, and Δ valleys, respectively. The room temperature total mobility at $x = 0.895$ is 0.13 that of pure Ge, or 0.38 that of pure Si. The factor $\frac{dr_i}{d\epsilon}$ is 97, -53 , and -44 , and $\frac{d\mu_i}{d\epsilon}/\mu$ is 553, -36 , and -8 for the $L3$, $L1$, and Δ valleys, respectively. Adding up all these factors in Eq. (4) yields the gauge factor $G = 400$ at $x = 0.895$ and zero pre-strain in Fig. 2. In this case, most of the gauge factor is due to the $L3$ valley terms. The $L1$ and Δ terms have the opposite sign, and therefore reduce the gauge factor, but are very small in comparison. We also note that both the change in occupation and intervalley scattering, viz., the first and second terms in Eq. (4), contribute substantially to G , with 185 and 245, respectively.

At very low temperatures, because the Fermi distribution is so sharp, the gauge factors are much larger. However, they also vary abruptly with both strain and alloy composition, remaining high for a very narrow range of strains. Doping may reduce the temperature dependence and sensitivity to strain, at the cost of lowering the gauge factor.²⁷

IV. CONCLUSION

To conclude, we have used computational *ab initio* methods to explore the strain-composition-current parameter space in silicon-germanium alloys to find the largest possible piezoresistive effect. We found room-temperature strain gauge factors as large as 500, and as high as 135 000 at cryogenic temperatures. The room temperature gauge factor is 300% larger than that for single crystalline silicon, and twice as large as the latest value reported in nanowires. We should note that to achieve such large gauge factors in SiGe, the alloy composition must be controlled to within 3%. In addition, gauge factors are not constant at all ranges of strain, especially at low temperatures. The effects of doping to stabilize the temperature dependence of the gauge factor should also be considered. However, we hope that the gauge factors reported here together with the compatibility of silicon germanium with the current fabrication technology will provide a new and cheap way to improve the sensitivity of piezoresistance-based sensors.

ACKNOWLEDGMENT

This work has been funded by Science Foundation Ireland.

¹W. Thomson, *Proc. R. Soc. London* **8**, 550 (1856).

²D. Clark and G. Datwyler, *Proc. Am. Soc. Test. Mat.* **38**, 98 (1938).

³C. S. Smith, *Phys. Rev.* **94**, 42 (1954).

⁴A. A. Barlian, W.-T. Park, J. R. Mallon Jr., A. J. Rastegar, and B. L. Pruitt, *Proc. IEEE* **97**, 513 (2009).

⁵K. Terauds, P. E. Sanchez-Jimenez, R. Raj, C. Vakifahmetoglu, and P. Colombo, *J. Eur. Ceram. Soc.* **30**, 2203 (2010).

⁶W. D. Edwards and R. P. Beaulieu, *J. Phys. E* **2**, 613 (1969).

⁷P. Gonzalez, L. Haspeslagh, K. De Meyer, and A. Witvrouw, in *Proceedings of 23rd IEEE International Conference on MEMS* (IEEE, Piscataway, 2010), p. 580.

⁸A. C. H. Rowe, A. Donoso-Barrera, Ch. Renner, and S. Arscott, *Phys. Rev. Lett.* **100**, 145501 (2008).

⁹P. Neuzil, C. C. Wong, and J. Reboud, *Nano Lett.* **10**, 1248 (2010).

- ¹⁰J. S. Milne, A. C. H. Rowe, S. Arscott, and Ch. Renner, *Phys. Rev. Lett.* **105**, 226802 (2010).
- ¹¹A. Koumela *et al.*, *Nanotechnology* **22**, 395701 (2011).
- ¹²R. W. Keyes, *J. Phys. Chem. Solids* **3**, 102 (1957).
- ¹³F. Murphy-Armando and S. Fahy, *Phys. Rev. Lett.* **97**, 096606 (2006).
- ¹⁴S. Joyce, F. Murphy-Armando, and S. Fahy, *Phys. Rev. B* **75**, 155201 (2007).
- ¹⁵F. Murphy-Armando and S. Fahy, *Phys. Rev. B* **78**, 035202 (2008).
- ¹⁶F. Murphy-Armando and S. Fahy, *J. App. Phys.* **110**, 123706 (2011).
- ¹⁷A. Druzhinin *et al.*, *Cryst. Res. Tech.* **37**, 243 (2002).
- ¹⁸A. Franceschetti and A. Zunger, *Nature (London)* **402**, 60 (1999).
- ¹⁹F. Murphy-Armando and S. Fahy, *J. App. Phys.* **109**, 113703 (2011).
- ²⁰V. G. Tyuterev, S. V. Obukhov, N. Vast, and J. Sjakste, *Phys. Rev. B* **84**, 035201 (2011).
- ²¹J. Sjakste, N. Vast, and V. G. Tyuterev, *Phys. Rev. Lett.* **99**, 236405 (2007).
- ²²C. Jacoboni and L. Reggiani, *Rev. Mod. Phys.* **55**, 645 (1983).
- ²³D. Chattopadhyay and H. Queisser, *Rev. Mod. Phys.* **53**, 745 (1981).
- ²⁴R. Barrie, *Proc. Phys. Soc. London, Sect. B* **69**, 553 (1956).
- ²⁵P. Yu and M. Cardona, *Fundamentals of Semiconductors* (Springer, Berlin, 2001).
- ²⁶H. Rolnick, *Phys. Rev.* **36**, 506 (1930).
- ²⁷O. N. Tufte and E. L. Stelzer, *J. Appl. Phys.* **34**, 313 (1963).